Finite Element Simulation of Laser Cladding for Tool Steel Repair

Santanu Paul, Ramesh Singh and Wenyi Yan

Abstract Laser cladding is a coating technique, wherein several layers of clad materials are deposited over a substrate so as to enhance the physical properties of the work-piece such as wear resistance, corrosion resistance etc. Strong interfacial bond with minimum dilution between the material layers is a pre-requisite of the process. This technique also finds widespread applications in repair and restoration of aerospace, naval, automobile components. A thermomechanical finite element models is developed wherein the Gaussian moving heat source is modelled along with element birth and death technique to simulate powder injection laser cladding of CPM9V over H13 tool steel, which is extensively used for repair of dies. The present work focuses on predicting the clad geometry and other clad characteristics such as the heat affected zone, dilution region and the subsequent residual stress evolution. It is expected that this knowledge can be used for repair of structures subjected to cyclic thermomechanical loads.

Keywords Finite element model · Gaussian laser heat source · Element birth technique · Laser cladding

S. Paul (✉)
IIT B-Monash Research Academy, Mumbai 400076, India
e-mail: santanupaul@iitb.ac.in

R. Singh
Indian Institute of Technology, Mumbai 400076, India
e-mail: ramesh@me.iitb.ac.in

W. Yan
Monash University, Clayton VIC3800, Australia
e-mail: wenyi.yan@monash.edu

S.N. Joshi and U.S. Dixit (eds.), *Lasers Based Manufacturing*,
Topics in Mining, Metallurgy and Materials Engineering,
DOI 10.1007/978-81-322-2352-8_9

1 Introduction

The high cost components used in the automobile/aerospace industry are sometimes operated beyond their original design life during, which they are subjected to cyclic/repeated thermomechanical loading thereby causing fatigue, corrosion and wear (Liu et al. 2011). Such age-related problems during service are common initiators of failures that cause high-performance and high-value components to be rendered useless (Pinkerton et al. 2008). Therefore, repair/restoration of such worn out or damaged high cost components used in the automobile/aerospace industry becomes beneficial as it can drastically reduce the overall cost multiple times by further extending the service life of these components (Wang et al. 2002).

Alternatively, the introduction of new forming materials like High Strength Steels (HSS), such as H13 tool steels (used mainly in the automotive sector) have introduced new challenges in tool manufacturing and repair of dies/moulds to the cold and hot shaping industry. These HSS are extremely aggressive for tools and dies thereby forcing the die sector to use new powder metallurgical tool steels, with an excellent combination of toughness, hardness and wear resistance for cutting, deep-drawing and bending dies (Leunda and Soriano 2011). A group of high vanadium-containing tool steels (such as CPM9, 10 and 15V), produced via powder metallurgy have proven to be successful in achieving high yield strength with high elongation and considerable work hardening along with excellent wear resistance during forming of HSS (Wang et al. 2006).

The moulds and dies used in hot and cold working industry are subjected to cyclic/repeated thermomechanical loading and thereby undergo wear and other localized damage. This calls for a repair process that does not induce tensile residual stresses. Traditional thermal spraying, Tungsten Inert Gas, Gas Metal Arc welding (GMAW) or High Velocity Oxygen Fuel (HVOF) techniques cannot be used effectively for powder metallurgical steels due to thermal damage and the process inaccuracies. On the other hand, these dies have very complex 3-D shape and very precise contoured deposition is required for the repair of such components. Moreover, repair being a localized process requires smaller beam size and precision. Therefore, it is imperative that the substrate properties should not deteriorate due to the heat affected zone and/or dilution. In this regard, a laser-based deposition technology such as laser cladding is a promising technique, in the remanufacturing industry, as it is characterized by localized and rapid fusion of materials. As a result, a relatively narrow Heat Affected Zone (HAZ) is generated.

Laser cladding is a material deposition technique in which the metallic materials in powdered form are supplied into a laser generated heat spot, by means of a carrier gas, where the material melts and forms a melt pool, which quickly solidifies into metal layers. As the metal powder passes through the laser beam, it is melted and deposited in the melt pool created by the laser beam on the metal substrate. By completely fusing the feedstock material, metal powders are directly transformed into fully dense solid objects composed of metallurgical bonded tracks of material that require no final finishing. In addition, laser cladded material exhibits

mechanical properties equivalent to those of similar alloys in the wrought condition. Partial overlapping of individual tracks in a suitable pattern produces a continuous layer of material. By overlapping such layers, fully dense and metallurgically sound 3D objects are generated (Costa and Vilar 2009).

The aim of laser surface cladding is to deposit a coating material, with required properties, on to different metallic substrates in such a way as to produce a good metallurgical bonding with the substrate to improve surface properties such as wear resistance, corrosion resistance, and high-temperature oxidation resistance. It is considered as a strategic technique, since it can yield surface layers that, compared to other hard facing techniques, have superior properties in terms of homogeneity, hardness and microstructure. Compared to the conventional repair methods, laser cladding process yields minimum dilution of the cladded layer by the elements from the substrate or vice versa thereby resulting in a very small HAZ (Hu et al. 1998a, b; Mc Daniels et al. 2008). The relatively small HAZ therefore results in tiny deformation and stress along with high dimensional accuracy and integrity of the final products (Wang et al. 2002; Mc Daniels et al. 2008).

Conventional methods such as TIG/GMAW though relatively easy to apply, produce a lot of heat, thereby causing high residual stresses, resulting in distortion heat-related effects in the base metal (Tusek and Ivancic 2004). On the other hand alternative techniques such as plasma transferred arc (PTA) welding (Su et al. 1997) and electron beam (EB) welding (Henderson et al. 2004), although gives very precise heat flux, require complex and expensive apparatus. The high velocity oxy-fuel (HVOF) thermal spraying technique (Tan et al. 1999) procedure which finds widespread applications in many industries produces less component distortion than with TIG welding and it has many advantages over plasma spraying, including deposition of a thicker and lower-porosity coating. However, tight control of depth and spread of deposited material is not possible, which necessitates machining for finishing stage. In comparison, laser cladding due to its localized heat affected zone, flexibility and precise control over the deposition area, produces lower residual stress than from TIG welding based repair. The process can induce desirable compressive residual stresses at the surface (Grum and Slabe 2003; Moat et al. 2007). The physical and corrosion properties of the clad material can be difficult to predict because it undergoes a repeated heating–cooling cycle (Pinkerton et al. 2006), but in many cases clad properties are superior to those of the parent material (Majumdar et al. 2005).

In addition to the surface coating applications, due to a localized heat affected zone, flexibility and precision, powder deposition by laser cladding has a vast scope in repair of worn out aerospace structures, gears and dies/moulds for various manufacturing operations with little distortion and intermixing as compared with plasma powder/TIG build-up welding and thermal spraying techniques (Steen 2003). Repair of power station turbine blades (Brandt et al. 2009), engine valve seats (Kawasaki et al. 1992) and other components using LC have been reported in literature (Liu et al. 2011). For laser cladding of high-alloy tool steels such as H13 tool steels, cracking often occurs in the coating as a result of thermal and/or phase-transformation stresses thereby restricting the applications of these tool steels in

laser cladding. Pre-heating of the matrix has been used to eliminate cracking of the coating (Zhang et al. 2001). However, this reduces the cooling rate and, thereby, affecting the microstructure of the cladding. On the other hand, a group of high vanadium-containing tool steels (such as CPM9, 10 and 15V), produced for powder metallurgy application, capable of producing high yield strength with high elongation and considerable work hardening along with excellent wear resistance (Wang et al. 2006) can be used as cladding materials for anti-wear applications. In fact, studies have been reported on laser cladding with CPM10V (Hu et al. 1998a, b) and other high vanadium tool steels (Zhang et al. 1999).

Residual stresses are produced in the parts produced by laser powder deposition techniques such as laser cladding due to the thermal history dependence phenomena in such processes. Residual stresses in clad material could affect the component's resistance to corrosion and fatigue cracks due to high thermal stress concentration (Sun et al. 2012). Therefore, the control of residual stresses plays a significant role in determining the mechanical performance of the fabricated parts which can be conveniently analysed by using modelling techniques. Although the interaction between certain phase transformations and the stress field are known and have been studied and modelled by researchers working on other heat treatment processes, such interaction has only been analysed briefly in the context of laser powder deposition (Griffith et al. 1998; Ghosh and Choi 2005, 2006, 2007).

One of the pre-requisites of laser cladding process is to keep dilution to a minimum to minimize the mixing between the clad layer and the substrate in order to maintain the properties of the baseline material (Steen 2003). However, high dilution allows stronger bonding between the clad and base material and in some case may have beneficial properties (Schneider 1998). Therefore the weakest point in a laser cladded component is the clad/HAZ interface due to inconsistent dilution/fusion (Mc Daniels 2008; Schneider 1998; Pinkerton et al. 2008). In the HAZ, the substrate material is heated to a temperature below the melting temperature and cooled at a lower rate than the coating surface. This trend can lead to microstructural changes in the HAZ that are difficult to control and could have a detrimental effect on the mechanical properties of the part (Mc Daniels et al. 2008). Cracks in laser-welded, high-strength, low-alloy steels formed near the borderline of the fusion line and the HAZ have been reported by Onoro and Ranninger (1997) with fatigue resistance minimum in the HAZ near the fusion line (Lee et al. 2000).

Finite element modelling is an appropriate tool to predict the temperature field, heat affected zone (HAZ), dilution zone and residual stress developed, so as to predict the clad quality and to develop optimum and successful cladding conditions. Previous efforts in developing sequential thermomechanical models provide temperature profile and cooling rate to predict the microstructure of the substrate (Wang et al. 2006; Picasso et al. 1994; Huan et al. 2006). In addition to this a few studies reported in the literature have also considered molten metal flow and phase transition (Wang et al. 2006). However, the finite elements models to evaluate the temperature profile for powder injection technique have been developed with constant convection co-efficient which may introduce errors (Liu et al. 2011; Wang et al. 2002; Shi and Qianchu).

Most modelling efforts focus their attention on phenomena occurring during the deposition of a single track of material or the build-up of thin wall geometry by overlapping several single pass layers. Not only does the thin wall geometry represent the simplest case of multilayer laser powder deposition, it is also the one that requires least effort to create a numerical representation of the problem (Amon et al. 1998) and the one that (potentially) requires less computation time and disk storage space.

Sequential thermomechanical analysis of laser cladding process in ANSYS® has been performed to obtain temperature profile for both planar and curved mesh of clad profile (Chen and Xue 2010; Deus and Mazumder 2006; Zhang et al. 2008, 2011; Plati et al. 2006). The temperature values obtained from transient thermal analysis are used as input for obtaining longitudinal and shear residual stresses for the thermomechanical analysis (Chen and Xue 2010; Deus and Mazumder 2006; Zhang et al. 2008, 2011; Plati et al. 2006) for various material systems, such as, copper on aluminium (Crespo et al.), Stellite on austenitic stainless steel AISI 304 (Suarez et al. 2010) and Monel on Ni-based alloys (Chunhua et al. 2012).

As noted previously, most of the laser cladding work reported is for non-powder metallurgical materials which are not very applicable for die repairs. However, thermomechanical model to investigate the HAZ, dilution zone and residual stress developed and thereby predict the clad quality have been reported in literature (Chunhua et al. 2012) for deposition of CPM9V on H13 tool steel. As a whole the finite element models available in literature (Plati et al. 2006; Paul et al. 2014) simulate the addition of new clad elements to the substrate using the element birth technique with the clad elements being deposited at the solidus temperature of the substrate, and therefore lack the ability to predict the clad geometry for the process. Consequently, this work is focused on the development of a 3-D coupled thermomechanical finite element modelling in ABAQUS® for laser cladding of CPM9V (crucible steel) on H13 tool steel. The addition of new elements to the substrate is simulated by using the element birth technique and the heat load addition is simulated by writing a user defined subroutine DFLUX in ABAQUS®. The clad geometry, clad dilution, heat affected zone and the residual stresses have been predicted from the model and compared with the experimental results (Paul et al. 2014).

2 Process Modelling

2.1 Physical Description of Process

In this work, the *powder injection* mode of laser cladding is considered. In this technique of laser cladding the powdered material is injected from a nozzle and is deposited over the base material in the presence of a laser beam. The description of the process is elaborated schematically in Fig. 1.

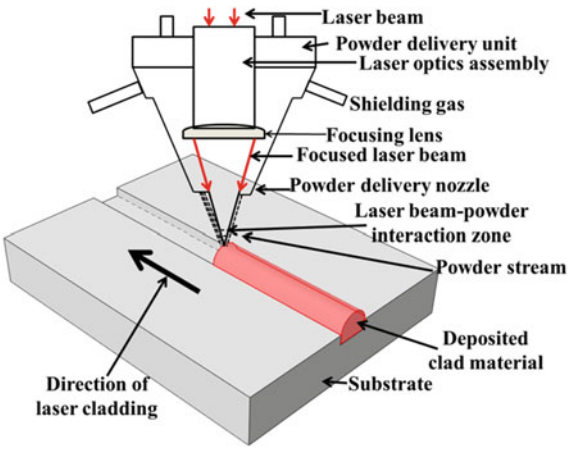

Fig. 1 Schematic of powder injection laser cladding technique

Table 1 Chemical composition of H13 tool steel (wt%)

C	Cr	Mn	Mo	Si	S	V
0.39	5.2	0.4	1.4	1.1	0.003	0.95

Data source Chen and Xue (2010)

Table 2 Chemical composition of CPM9V (wt%)

C	Cr	Fe	Mo	V
1.2	5.250	82.54	1.3	9.10

Data source Chen and Xue (2010)

In this work the substrate employed is H13 tool steel and clad material is vanadium carbide steel, CPM9V, extensively used for repair of damaged/worn out dies. Chemical composition of H13 tool steel is provided in Table 1 and the chemical composition of CPM9V is listed out in Table 2.

The actual cladding with dimension of substrate as 125 mm × 105 mm × 15 mm over which clad was deposited at length of 40 mm has been obtained from literature (Crespo et al.). Gaussian laser heat source is employed with beam diameter of 3 mm and power of 2000–3800 W. Powder particles was spherical in shape with size of 44–104 μm. In the current work a coupled thermomechanical finite element models of powder injection technique of laser cladding with Gaussian moving heat source is developed. The coupled thermomechanical model developed predicts the clad quality for laser power of 1700 W, feed rate of 5 g/min, scanning speed of 200 mm/min and beam diameter of 3 mm.

2.2 Model Assumptions

The following assumptions are made about the process for developing the coupled thermomechanical model:

- Stationary frame of reference has been attached with the laser beam, considering that the dimensions of the work-piece are large compared to those of the molten pool.
- Heat transfer in the process is assumed to occur without any internal heat generation and the variation of heat transfer co-efficient with temperature is neglected.
- Gaussian moving heat source with linear decrease of heat input with penetration depth is assumed.
- Fluid flow in the melt pool and its subsequent effect on the heat transfer co-efficient is neglected.
- Body force and surface traction are neglected in thermomechanical analysis and only the loading due to transient thermal field (Gaussian moving heat source) on the body is considered.
- For residual stress analysis elastic perfectly plastic behaviour with temperature dependent yield stress, with no work hardening and prior strain history effects are assumed.
- Creep (time dependent deformation) effects are also neglected.

2.3 Governing Equations

In a coupled thermomechanical finite element analysis of laser cladding the values of nodal temperature obtained after thermal analysis of Gaussian moving heat laser source are used as input to calculate the mechanical response in particular the residual stresses developed. Transient heat conduction equation is used as the basic governing equation for thermal analysis which is given as:

$$\frac{\partial}{\partial x}\left(k\frac{\partial T}{\partial x}\right)+\frac{\partial}{\partial y}\left(k\frac{\partial T}{\partial y}\right)+\frac{\partial}{\partial z}\left(k\frac{\partial T}{\partial z}\right)+\mathrm{Q}=\rho \mathrm{C_p}\frac{\partial T}{\partial \mathrm{t}}+\rho U_x C_p\frac{\partial T}{\partial x} \quad (1)$$

where ρ, C_p and k refers to density, specific heat and thermal conductivity respectively of material; T and t refer to the temperature and time variables respectively.The thermal stresses in a clad-substrate system are developed due to the presence of relatively high thermal gradients between dissimilar materials. The relatively high thermal gradient between dissimilar materials in general develops due to the fact that, the clad and substrate materials have different coefficients of thermal expansion and different reference temperatures. As laser cladding is a much localized process therefore, during a short interval of time, a thin layer of the

substrate is heated up to the melting point, and a molten layer of the clad material is deposited on it. Thereafter, the heat is conducted into the substrate and the clad solidifies and starts shrinking due to thermal contraction, whereas the substrate first expands and later contracts according to the local thermal cycle. Hence, the residual stresses are evaluated as a function of time, when after heating the work-piece is left to cool under normal conditions and stress is analysed after infinite time period. Therefore, in the thermomechanical analysis of the process the only loading on the system due to the transient thermal field is considered, as any external loading, body force and surface traction are neglected. Thus, the strain–displacement relation is given by:

$$\in_{ij} = \frac{du_i}{dx_j} + \frac{du_j}{dx_i} \tag{2}$$

where σ_{ij} is stress tensor, n_{ij} is exterior normal to surface, u_1 is displacement and $\in_{ij}$ is total strain tensor, where the total strain $\in_{ij}$ is given by:

$$\in_{ij} = \in_{ij}^{el} + \in_{ij}^{p} + \in_{ij}^{th} \tag{3}$$

where $\in_{ij}^{el}$ represents elastic strain, $\in_{ij}^{p}$ represents plastic strain and $\in_{ij}^{th}$ is the thermal strain. The stress and elastic strains are connected through elastic moduli or stiffness tensor C_{ijkl}. For isotropic material stiffness tensor is function of Young's modulus, E and Poisson's ratio, υ given by:

$$\sigma_{ij} = C_{ijkl}\left(\in_{ij} - \in_{ij}^{th} - \in_{ij}^{p}\right) \tag{4}$$

The thermal strains are given by:

$$\in_{ij}^{th}(T) = \alpha_T(T)\left(T - T_{ref}\right) - \alpha_T(T_0)\left(T_0 - T_{ref}\right) \tag{5}$$

where α_T is coefficient of thermal expansion, T_{ref} is reference temperature (i.e., starting temperature from which coefficient of thermal expansion is obtained) and T_0 is initial temperature.

Besides these the following initial and boundary conditions are also satisfied:

$$T(x, y, 0) = T_0 \tag{6}$$

$$T(x, y, \infty) = T_0 \tag{7}$$

2.4 Numerical Formulation

For simulation a half symmetric model with dimension 6 mm × 6 mm × 6 mm has been developed. Coupled analysis for thermal and mechanical phenomena is considered. To evaluate the effect of thermal stresses produced during the process 8-node coupled temperature-displacements, C3D8RHT reduced integration elements are used. Mesh size of 54 µm × 100 µm × 100 µm has been considered across the cross-section of the clad, whereas in the substrate 46 µm × 100 µm × 100 µm. Figure 2 presents a pictorial representation of the model geometry along with the dimensions and meshed geometry. Total number of node is 27,510 and total number of elements is 24,820.

In powder injection technique, the continuous addition of material or mass on to the substrate is modelled by representing geometry of finite elements that change over time so as to simulate the powdered nature of the material. This is achieved by means of successive discrete activation of new set of elements into the computational domain or geometry using element birth and death feature as illustrated by Fig. 3. Furthermore, as the heat source moves forward the elements activated in the previous set are deactivated so as to initialize the cooling process.

Along with the element birth–death technique used to simulate the effect of powder deposition, the Gaussian moving heat source is also modelled using the DFLUX subroutine in ABAQUS®. The Gaussian moving heat source with linear decrease of heat input with penetration depth is given by (Shanmugam et al. 2013):

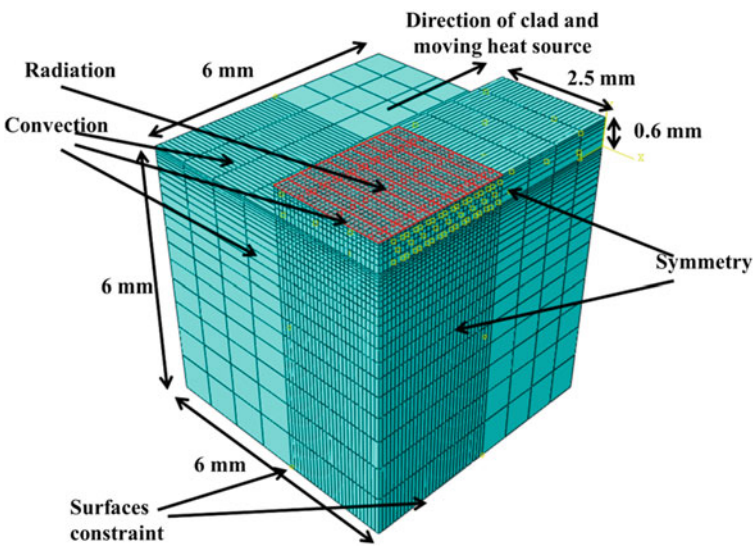

Fig. 2 Geometry of the model and mesh design along with the loading and boundary conditions

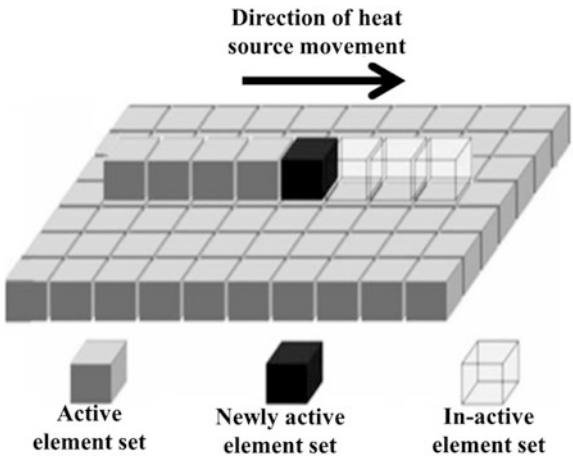

Fig. 3 Powder deposition modelled by element birth technique

$$Q(r,z) = \frac{Q_L}{\pi r_0^2 d} \exp\left[\left(1 - \frac{r^2}{r_0^2}\right)\left(1 - \frac{z}{d}\right)\right] \tag{8}$$

where Q_L is the laser power, r_0 is the beam radius, d is the heat penetration depth and r the instantaneous laser beam location given by:

$$r^2 + x^2 + y^2 + z^2 \tag{9}$$

where x, y, z are the co-ordinates of the laser heat source at time t.

While applying this technique to the model, initial volume of powder deposited is calculated using the feed rate. The height and width of powder thus obtained is deposited in each time step, and value of time step is set accordingly. Thereafter as the Gaussian moving heat source scans the surface, the clad and a thin substrate layer is melted and a strong interfacial bond is formed. The elements then lose heat mainly by conduction into work-piece and heat loss is also by convection and radiation.

2.5 Loading and Boundary Conditions

Gaussian distribution of laser power with linear decrease of heat input with penetration depth given by Eq. (8) is considered to be emitted from the source. Boundary conditions like convective heat transfer (with heat transfer coefficient of 15 $Wm^{-2}\,K^{-1}$) and radiative heat transfer (with emissivity 0.3) results in heat losses from surfaces.

Subsequently, the associated initial conditions for three-dimensional thermal analysis are given by Eq. (6). The addition of clad to the substrate is modelled using element birth-death technique as depicted in Fig. 3. The reactivation of the cladding

elements is followed by the release of latent heat during solidification of the clad. After the activation of all the cladding elements, external heat injection is continued as the heat source moves forward, but the thermal analysis is continued until the system reached a steady state.

The rest of the work piece surfaces are open to atmosphere and are subjected to convective and radiative heat losses as depicted in Fig. 2. The above boundary condition is stated mathematically as:

$$K_n \frac{dT}{dn} + h(T - T_0) + \sigma \in \left(T^4 - T_0^4\right) = 0 \tag{10}$$

where n denotes the direction normal to surface, k_n refers to thermal conductivity; h, $\in$, σ and T_0 refers to surface heat transfer co-efficient, emissivity, Stefan-Boltzmann constant and ambient temperature respectively. The first term represents heat loss due to conduction from the surface whose unit normal is n. The second and third term refers to convection and radiation heat losses from the surface of the work-piece.

For the mechanical analysis external loading is not considered and to prevent the rigid body motion the nodes on the base are fully constrained to prevent elemental motion. The application of thermal load as Gaussian moving heat flux and the mechanical boundary conditions showing the surfaces which are fully constrained are illustrated in Fig. 3.

2.6 Material Properties

Temperature dependent thermo-physical properties are considered for both clad and substrate as these properties changes with temperature. Along with thermal properties like thermal conductivity, specific heat and latent heat, mechanical properties namely co-efficient of thermal expansion, young's modulus, poison's ratio and yield strength are provided as input. Stress and strain fields are dependent on evolution of plastic strains so kinematic hardening in addition to Von Misses yield criteria is assumed which is valid for clad, interface and the substrate region.

The yield strength as a function of temperature, decreases exponentially with temperature and tends to zero as the nodal temperature approaches the liquidus temperature. Accordingly, the "anneal temperature" feature in ABAQUS® is used which resets stress and strain values above molten temperature to zero. Also a very low value of Young's modulus is considered to make the melting zone a stress free zone.

Initially zero stress is considered in the material and then analysis is performed for residual stress by considering elastic perfectly plastic behaviour. The properties of CPM9V (clad) are listed in Table 3 and the thermo-physical properties of H-13 (substrate) are listed in Table 4.

Table 3 Thermo-physical properties of CPM9V mixture (Chen and Xue 2010)

Temperature (K)	Conductivity(W m^{-1} K^{-1})	Expansion (K^{-1})	Density (kg m^{-3})
300	20.48	1.102×10^{-5}	7455
373	21.6	1.105×10^{-5}	–
573	25.25	1.141×10^{-5}	–
820	26.08	1.186×10^{-5}	–

Other material properties of CPM9V used in the simulation are as follows (Chen and Xue 2010)
Melting temperature: 1773 K
Young's modulus: 221 GPa
Poisson's ratio: 0.28
Yield stress: 1600 MPa

Table 4 Thermo-physical properties of H13 tool steel (Chen and Xue 2010)

Temperature (K)	Conductivity (W m^{-1} K^{-1})	Expansion (K^{-1})	Density (kg m^{-3})
310	25	1.09×10^{-5}	7600
400	–	1.1×10^{-5}	–
500	26.3	1.15×10^{-5}	–
810	28	1.24×10^{-5}	–
900	–	1.31×10^{-5}	–
1000	30	–	–
1200	32	–	–
1500	35	–	–

Other material properties of H-13 used in the simulation are as follows (Chen and Xue 2010)
Melting temperature: 1730 K
Young's modulus: 210 GPa
Poisson's ratio: 0.3
Yield stress: 1400 MPa

3 Results and Discussion

The coupled thermomechanical analysis of cladding process is based on the fact that the temperature field obtained from the thermal analysis serves as the basis for prediction of clad geometry, the clad dilution and HAZ. Furthermore, for mechanical analysis as no external loading is considered apart from the application of thermal load as moving heat flux the prediction of thermal field for residual stress analysis becomes imperative.

3.1 Temperature Field

Figure 4a shows the contour plot of nodal temperature as the clad is being deposited. The red portion depicts the burnt away clad materials for a laser power of

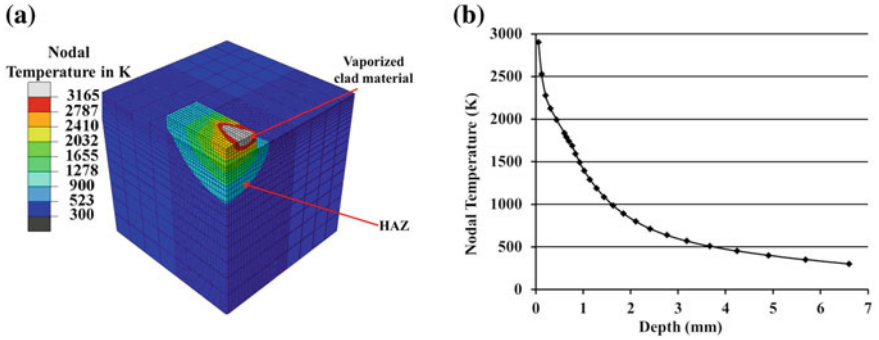

Fig. 4 **a** Contour of nodal temperature, **b** Variation of nodal temperature with depth

1700 W, feed rate of 5 g/min and scanning speed of 200 mm/min. The variation of nodal temperature along the cross-section of the clad when the laser beam is directly over the clad surface is shown in Fig. 4b. The finite element models developed calculates the clad height by eliminating the elements which have exceeded the vaporization temperature of the powder (CPM9V) from the computational domain. The comparison of the clad height as predicted by model shows a variation of 14 and 18 % variation for the prediction of clad width, from that of the experimental data (Plati et al. 2006). Therefore it is evident that the model is able to predict the clad geometry.

3.2 Results in Dilution and Heat Affected Zone

Dilution is the contamination of cladding with the substrate material which is detrimental to the clad quality. Therefore it is a pre-requisite to obtain clad with minimal dilution. However, it is very difficult to eliminate dilution but can be significantly reduced by selecting optimum parameters. For finite element analysis it is assumed that the part of the substrate that has melted typically results in dilution. Therefore, the molten depth of substitute can be used as a good estimate of dilution depth. Figure 5a compares the dilution value for the current model with that actually obtained through experiment (Paul et al. 2014). Figure 5a also compares the dilution as obtained for a coupled finite element models available in literature with thermal boundary condition (Paul et al. 2014). The current model predicts dilution with a variation of 25 % from the experimental which shows that the model is able to capture dilution that occurs during the process.

In the present work, the region between substrate melting temperature and 1000 K is considered as the Heat Affected Zone (HAZ) as illustrated by Fig. 4a. Figure 5b compares the HAZ value for the model and that actually obtained through

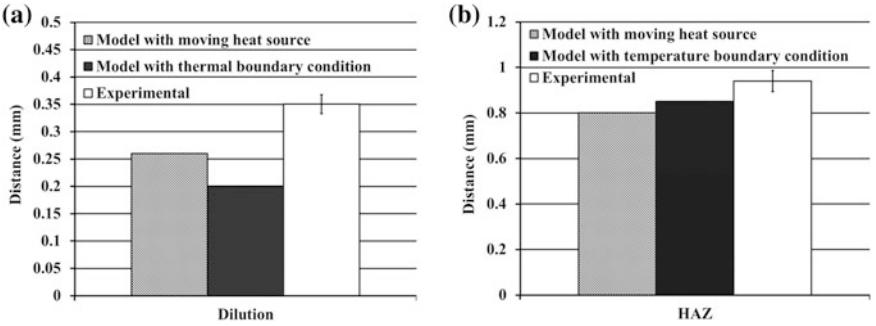

Fig. 5 Comparison of **a** dilution zone, **b** HAZ

experiments (Paul et al. 2014). The current model is able to predict the HAZ with a variation of 15 %. Thus it can be concluded that through the model both dilution and heat affected zone are being captured.

3.3 Residual Stress Analysis

As discussed in previous section in a clad-substrate system the presence of relatively high thermal gradients between dissimilar materials leads to the development of thermal stresses because of the presence of different co-efficient of thermal expansion and different reference temperatures for the clad and substrate materials. Due to laser cladding being a localized heating application during a short time interval, a thin layer of substrate is heated up to the liquidus temperature and a molten layer of the clad material is deposited on it. Thereafter, the heat is conducted into the substrate and the clad solidifies and starts shrinking due to thermal contraction, whereas the substrate first expands and later contracts according to the local thermal cycle which leads to the development of residual stresses.

The residual stress contour in the longitudinal direction, i.e., along the cladding direction is shown in Fig. 6a. The model predicts compressive stresses on the surface of the clad which originates to counter the tensile stresses induced at the interface because of high thermal contraction. The interface region contracts rapidly due to the rapid heat transfer to the relatively cooler substrate underneath whose dimensions do not change significantly, thereby inducing tensile stresses as the substrate.

Experimental values of longitudinal stresses were obtained through X-ray diffraction (XRD) technique (Paul et al. 2014) using a X-ray beam of diameter 500 µm. Figure 6b compares the model average values which are typically the nodal values averaged over an area of 500 µm. The model predicts a variation of 12 % in the residual stress in the longitudinal direction on the clad-substrate

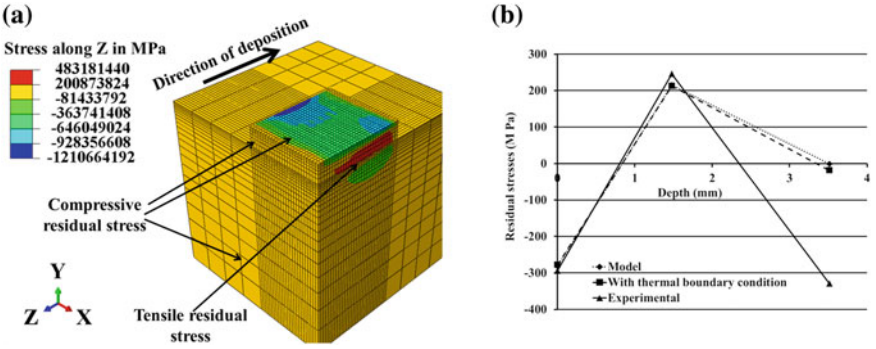

Fig. 6 **a** contour of residual stress along longitudinal direction, **b** comparison of residual stress along the direction of clad

interface. However, the development of compressive residual stress in the clad highlights the potential application of the process for in situ repair applications for die and aerospace components.

4 Conclusions

A coupled thermomechanical finite element models of powder injection laser cladding technique has been developed and the model results have been compared with the available experimental results [43]. Following are the main conclusions drawn from the present work:

- The thermomechanical model for powder injection laser cladding process with moving Gaussian heat source is able to predict the clad geometry with prediction errors lying between 14 and 18 %.
- Thermal analysis of the process can predict the temperature profile which can be used to estimate the extent of dilution and heat affected zones. The prediction errors lie between 15 and 25 %.
- The longitudinal residual stress has been characterized for clad, interface and the substrate regions. The nodal average values for the model over an area of 500 μm qualitatively predicted similar nature with reasonable variation.
- The longitudinal stress in the interface region is tensile in nature which can be attributed to the rapid heat transfer and higher thermal contraction at the interface.
- The analysis of the process also highlighted the application of the technique for repair and restoration applications of various high cost components due to evolution of compressive stresses on the surface of the clad.

References

Amon, C. H., Beuth, J. L., Weiss, L. E., Merz, R., & Prinz, F. B. (1998). Shape deposition manufacturing with micro-casting: Processing, thermal and mechanical issues. *Journal of Manufacturing Science and Engineering, 120*, 656–665.

Brandt, M., Sun, S., Alam, N., Bendeich, P., & Bishop, A. (2009). Laser cladding repair of turbine blades in power plants: From research to commercialization. *International Heat Treatment and Surface Engineering, 3*, 105–114.

Chen, J., & Xue, L. (2010). Laser cladding of wear resistant CPM9V tool steel on hardened H13 substrate for potential automotive tooling applications. In *Materials Science and Technology 2010 Conference and Exhibition*, (pp. 2459–2470).

Costa, L., & Vilar, R. (2009). Laser powder deposition. *Rapid Prototyping Journal, 15*, 264–279.

Da Sun, S., Liu, Q., Brandt, M., Janardhana, M., Clark, G. (2012). Microstructure and mechanical properties of laser cladding repair of AISI 4340 steel, 28th International Congress of the Aeronautical Sciences.

Deus, A., Mazumder, J. (2006). Three-dimensional finite element models for the calculation of temperature and residual stress fields in laser cladding. In *Laser Materials Processing Conference, ICALEO 2006 Congress Proceedings* (pp. 496–505).

Ghosh, S., & Choi, J. (2005). Three-dimensional transient finite element analysis for residual stresses in the laser aided direct metal/material deposition process. *Journal of Laser Applications, 17*, 144–158.

Ghosh, S., & Choi, J. (2006). Modeling and experimental verification of transient/residual stresses and microstructure formation in multi-layer laser aided DMD process. *Journal of Heat Transfer, 128*, 662–679.

Ghosh, S., & Choi, J. (2007). Deposition pattern based thermal stresses in single-layer laser aided direct material deposition process. *Journal of Manufacturing Science and Engineering, 129*, 319–332.

Griffith, M. L., Schlienger, M. E., Harwell, L. D., Oliver, M. S., Baldwin, M. D., Ensz, M. T., et al. (1998). Thermal behavior in the LENS process. In D. Bourell, J. Beaman, R. Crawford, H. Marcus, & J. Barlow (Eds.), *Paper presented at Solid Freeform Fabrication Symposium*. Austin, TX: University of Texas at Austin.

Grum, J., & Slabe, J. M. (2003). A comparison of tool-repair methods using CO_2 laser surfacing and arc surfacing. *Applied Surface Science, 208–209*, 424–431.

Henderson, M. B., Arrell, D., Larsson, R., Heobel, M., & Marchant, G. (2004). Nickel based superalloy welding practices for industrial gas turbine applications. *Science and Technology Welding and Joining, 9*, 13–21.

Hu, Y. P., Chen, C. W., & Mukherjee, K. (1998a). Development of a new laser cladding process for manufacturing cutting and stamping dies. *Journal of Materials Science, 33*, 1287–1292.

Hu, Y., Chen, C., & Mukherjee, K. (1998b). Innovative laser-aided manufacturing of patterned stamping and cutting dies: Processing parameters. *Materials and Manufacturing Processes, 13*, 369–387.

Kawasaki, M., Takase, K., Kato, S., Nakagawa, M. & Mori, K. (1992). Development of engine valve seats directly deposited onto aluminium cylinder head by laser cladding process, SAE Technical Paper Series, SAE Paper No. 920571. *SAE International, Warrendale, PA*, pp. 1–15.

Lee, H. K., Kim, K. S., & Kim, C. M. (2000). *Engineering Fracture Mechanics, 66*, 403–419.

Leunda, J., & Soriano, C. (2011). Laser cladding of vanadium-carbide tool steels for die repairs. *Proceedings of the Sixth International WLT Conference on Lasers in Manufacturing, physics procedia, 12*, 345–352.

Liu, Q., Janardhana, M., Hinton, B., Brandt, M., & Sharp, K. (2011). Laser cladding as a potential repair technology for damaged aircraft components. *International Journal of Structural Integrity, 2*, 314–331.

Majumdar, J. D., Pinkerton, A., Liu, Z., Manna, I., & Li, L. (2005). Mechanical and electrochemical properties of multiple-layer diode laser cladding of 316L stainless steel. *Applied Surface Science, 247*, 373–377.

Mc Daniels, R. L., White, S. A., Liaw, K., Chen, L., McCay, M. H., Liaw, P. K. (2008). Effects of a laser surface processing induced heat-affected zone on the fatigue behavior of AISI 4340 steel. *Materials Science and Engineering: A*, *485*, 500–507.

Moat, R., Pinkerton, A. J., Hughes, D. J., Li, L., Preuss, M., and Withers, P. J. (2007). Stress distributions in multilayer laser deposited Waspaloy parts measured using neutron diffraction. In *Proceedings of 26th International Congress on Applications of Lasers and Electro- optics (ICALEO).* Orlando, California, CD.

Onoro, J., & Ranninger, C. (1997). Fatigue behavior of laser welds of high-strength low-alloy steels. *Journal of Material Process and Technology, 68*, 68–70.

Paul, S., Ashraf, K., Singh, R. (2014). Residual stress modeling of powder injection laser surface cladding for die repair applications. In *Proceedings of the ASME 2014 International Manufacturing Science and Engineering Conference MSEC2014.* Detroit, Michigan, USA.

Picasso, M., Marsden, C.F., Wagniib.RE J.-D., Frenk, A., Rappaz, M. (1994). A Simple but realistic model for laser cladding, metallurgical and materials transactions B *25B*, p. 281.

Pinkerton, A., Wang, W., Li, L. (2008). Component repair using laser direct metal deposition. In *Proceedings of the Institution of Mechanical Engineers, Part B: Journal of Engineering Manufacture 222*, 827–836.

Pinkerton, A. J., Karadge, M., Syed, W. U. H., & Li, L. (2006). Thermal and microstructural aspects of the laser direct metal deposition of Waspaloy. *Journal of Laser Applications, 18*, 216–226.

Plati, A., Tan, J., Golosnoy, I., Persoons, R., Acker, K., & Clyne, T. (2006). Residual stress generation during laser cladding of steel with a particulate metal matrix composite. *Advance Engineering Materials, 8*, 619–624.

Qi, H., Mazumder, J., Ki, H. (2006). Numerical simulation of heat transfer and fluid flow in coaxial laser cladding process for direct metal deposition. *Journal of Applied Physics*, *100*, 024903.

Schneider, M. F. (1998). *Laser cladding with powder; Effect of some machining parameters on clad properties. Ph.D Thesis,* University of Twente, Enschede, The Netherlands.

Shanmugam, N. S., Buvanashekaran, G., Sankaranarayanasamy, K. (2013). Some studies on temperature distribution modelling of laser butt welding of AISI 304 stainless steel sheets. *World Academy of Science, Engineering and Technology 7*.

Steen, W. M. (2003). *Laser material processing* (3rd ed.). London: Springer.

Su, C. Y., Chou, C. P., Wu, B. C., Lih, W. C. (1997). Plasma transferred arc repair welding of the nickel-base superalloy IN-738LC. *Journal of Materials Engineering and Performance 6*, 619–627.

Suarez, A., Amado, J., Tobar, M., Yanez, A., Fraga, E., & Peel, M. (2010). Study of residual stresses generated inside laser cladded plates using FEM and diffraction of synchrotron radiation. *Surface and Coatings Technology, 204*, 1983–1988.

Tan, J. C., Looney, L., & Hashmi, M. S. J. (1999). Component repair using HVOF thermal spraying. *Journal of Materials Processing Technology, 92–93*, 203–208.

Tusek, J., Ivancic, R. (2004). Computer-aided analysis of repair welding of stamping tools. *Z. fu¨r Metallkunde*, *95*, 8–13.

Wang, J., Prakash S., Joshi Y., Liou F. (2002). Laser Aided Part Repair-A Review. In *Solid Freeform Fabrication Proceedings*, pp. 57–64.

Wang, S.-H., Chen, J.-Y., & Xue, L. (2006). A study of the abrasive wear behavior of laser-clad tool steel coatings. *Surface and Coatings Technology, 200*, 3446–3458.

Zhang, C. H., Hao, Y. X., Qi, L., Hu, F., Zhang, S., & Wang, M. C. (2012). Preparation of Ni-Base alloy coatings on monel alloy by laser cladding. *Advanced Materials Research, 472–475*, 313–316.

Zhang, P., Ma, L., Yuan, J., Yin, X., & Cai, Z. (2008). The finite element simulation research on stress-strain field of laser cladding. *Journal of Engineering Materials, 373–374*, 322–325.

Zhang, Y., Yuan, X., & Zeng, X. (1999). *ICALEO 1999: Laser materials processing conference* (p. 241). USA: San Diego.

Zhang, Y., Zeng, X., & Yuan, X. (2001). *ICALEO 2001: Applications of lasers and electro-optics* (p. 577). USA: Jacksonville.

Zheng, L., Xie, W., & Li, Y. (2011). The numerical simulation on the temperature field of laser cladding. *Journal of Engineering Materials, 467–469*, 1372–1376.